# Interaction of the Effector Domain of MARCKS and MARCKS-Related Protein with Lipid Membranes Revealed by Electric Potential Measurements†

Günther Bähr, Anke Diederich, Guy Vergères, and Mathias Winterhalter*

*Department of Biophysical Chemistry, Biozentrum of the University of Basel, Klingelbergstrasse 70, CH-4056 Basel, Switzerland*

*Received July 22, 1998; Revised Manuscript Received September 14, 1998*

ABSTRACT: We have investigated the binding of the effector domains of myristoylated alanine-rich C kinase substrate (MARCKS) and of MARCKS-related protein (MRP) to lipid model membranes. For membrane systems we used lipid monolayers on a Langmuir trough and black lipid membranes (BLM). The binding of the peptides was detected by monitoring changes in the boundary potential of the lipid membranes. The vibrating plate technique (VPT) and the method of inner field compensation (IFC) were used for the monolayer and for the BLM, respectively. We could show that the effector domain of MARCKS binds to acidic lipid membranes mainly via electrostatic interactions and to zwitterionic lipid membranes via hydrophobic interactions. Isobaric measurements on lipid monolayers revealed that binding of both effector domains is accompanied by partial insertion of the peptides into the membrane. Adsorption and insertion of the peptides could be followed simultaneously by the VPT and by recording the increase in area of the lipid monolayer, respectively. No temporal delay could be observed between adsorption and insertion of the peptides, demonstrating that adsorption is the rate-limiting step and that insertion is faster than the time resolution of the experiments, i.e., a few seconds. Both the IFC and the VPT did not show any significant difference between the behaviors of the effector domains of MARCKS and MRP. With the IFC we show that calcium can regulate the translocation of the MARCKS effector peptide between the membrane and calmodulin (CaM) in the bulk. Our results indicate, that the IFC and VPT are suitable qualitatively, and to a certain extent quantitatively, as membrane binding assays.

Electric fields play a major role in biological processes. At the cellular level the origin of these electric effects is mostly due to the presence of membranes which disrupt the homogeneity of the aqueous phase. Membranes can act as a selective barrier between electrolytes and consequently induce the formation of transmembrane potentials. This property has been widely used by electrophysiologists to investigate the mode of action of protein channels which regulate the ionic permeability of cellular membranes (*1*). Membranes also represent an interphase between the aqueous media, with the possible formation of surface potentials. For a review of the electrostatic properties of membranes see for example ref *2*. All membrane-bound proteins, including proteins which do not form channels, are expected to modify the surface potential to some extent. This phenomenon includes, for example, the binding of peripheral membrane proteins which often involves electrostatic interactions with phospholipid headgroups. In addition, conformational changes as well as posttranslational modifications (e.g., phosphorylation) of membrane-bound proteins are likely to affect the electric properties of membranes (*3*, *4*). To date, little attempt has been made to record directly the alteration of the electric properties of a membrane during protein binding. To take one step in that direction, we have investigated how peptides corresponding to the effector domains of the members of the myristoylated alanine-rich C kinase substrate (MARCKS)[1] protein family affect the electric potentials of planar membranes.

MARCKS proteins are involved in several cellular processes such as secretion, motility, mitosis, and transformation (*5*, *6*). In addition to their ability to interact with calmodulin and actin filaments, reversible binding to the plasma membrane is most certainly an important component of the function of these proteins. The MARCKS family comprises two proteins, MARCKS and MARCKS-related protein (MRP). MARCKS is a 30−35 kDa protein encoded by the *macs* gene. MRP is a 20 kDa protein encoded by the *mrp* gene. Although *macs* and *mrp* are ubiquitiously expressed, high levels of mRNA are found in brain (MARCKS and MRP) and in reproductive tissues (MRP).

Two domains mediate the binding of MARCKS proteins to lipid membranes. The N-terminal myristoyl chain inserts into the membrane (*7*). The effector domain in the middle

† This research was supported by the Swiss National Science Foundation (grant 3100-042045.94 to Professor Gerhard Schwarz, University of Basel).

* Address for correspondence: Dr. Mathias Winterhalter, Department of Biophysical Chemistry, Biozentrum, University of Basel, Klingelbergstrasse 70, 4056 Basel, Switzerland. Telephone: +41-61-267-2179. Fax: +41-61-267-2189. E-mail: winterhalter@ubaclu.unibas.ch.

[1] Abbreviations: MARCKS, myristoylated alanine-rich C kinase substrate; MRP, MARCKS-related protein; CaM, calmodulin; BLM, black lipid membranes; IFC, method of Inner Field Compensation; VPT, vibrating plate technique; DPhPC, diphytanoylphosphatidylcholine; DPhPS, diphytanoylphosphatidylserine; EGTA, ethylene glycol bis(β-aminoethyl ether) *N*,*N*,*N*′,*N*′-tetraacetic acid; MOPS, morpholinopropanesulfonic acid.

10.1021/bi981765a CCC: $15.00 
Published on Web 10/29/1998

```
          151
MARCKS:   Lys-Lys-Lys-Lys-Lys-Arg-Phe-Ser-Phe-Lys-Lys-Ser-Phe-
MRP:      Lys-Lys-Lys-Lys-Lys-------Phe-Ser-Phe-Lys-Lys-Pro-Phe-
          86

                                                    175
MARCKS:   Lys-Leu-Ser-Gly-Phe-Ser-Phe-Lys-Lys-Asn-Lys- Lys
MRP:      Lys-Leu-Ser-Gly-Leu-Ser-Phe-Lys-Arg-Asn-Arg-Lys
                                                    109
```

FIGURE 1: Amino acid sequence of MARCKS and MRP effector domains. Cationic amino acid residues are bold. Hydrophobic residues are underlined. Differences in the primary sequences of the two peptides are shown in italics.

of the MARCKS proteins contains 24−25 amino acid residues (Figure 1). Twelve to thirteen positively charged residues (Lys, Arg) contribute to the binding via electrostatic interactions with the headgroups of acidic phospholipids (*3*). In addition, six hydrophobic residues (Phe, Leu) also contribute to the binding by inserting into the membrane (*8*). Although both domains have been proposed to act cooperatively to firmly anchor MARCKS to lipid membranes (*3*), significant cooperativity was not observed with MRP (*7, 9*). In this work we study the binding of the effector domain of MARCKS and MRP to lipid model membranes. The adsorption of basic peptides corresponding to the effector domain of these proteins should reduce the negative surface charge density of membranes. In addition, the insertion of the hydrophobic residues of these peptides may lead to structural changes in the membrane, which may affect the membrane dipole potential.

In this work we investigated the modification of electric fields due to peptide binding. We adapted two methods, the IFC and VPT, to record electric fields at lipid membrane surfaces. Binding of biologically relevant molecules to lipid membranes has already been previously investigated with IFC (*10*, *11*) and with VPT (*12*−*15*). However, to our knowledge, both techniques have not been used in combination to study binding of peptides to membranes. Below we outline in some detail the concept, advantages, and difficulties of these techniques. We demonstrate the power of using these methods in conjunction by probing the binding of physiologically relevant peptides to lipid membranes.

In this paper, the concept of the boundary potential is fundamental. The boundary potential is the sum of surface potential and dipole potential for a lipid monolayer or for one leaflet of a BLM. For negatively charged lipids the surface potential is negative at the lipid surface and decreases in the aqueous solution as a function of distance from the membrane. The shape and magnitude of the surface potential near the membrane can be described by the Gouy−Chapman theory and depends on the surface charge density of the membrane and the composition of the electrolyte adjacent to the membrane (see Appendix).

In contrast to the surface potential, the origin of the dipole potential is not well understood. Earlier experiments with hydrophobic ions (*16*) have shown that the dipole potential leads to a positive potential inside the membrane which is usually significantly greater in magnitude than the surface potential. The dipole potential is altered if molecules with a different dipole moment insert into the membrane in a preferred orientation, or if changes in the structure of the membrane are induced. Oriented water molecules near the phospholipid headgroups may also contribute to the dipole potential. Furthermore, not only the origin of the dipole potential, but also its effect on membrane binding is not known to date.

A BLM consists of two adjacent monolayers, each layer having its own boundary potential. Under symmetrical conditions, both potentials are identical and the voltage drop across the hydrophobic core of the BLM is zero. A change in the surface or dipole potential on one side, for example following adsorption of peptides, leads to a voltage drop across the hydrocarbon region and therefore to Maxwell forces on the membrane. This can lead to changes in the thickness and therefore to changes in the membrane capacitance. In Materials and Methods we will show how this difference in boundary potentials can be measured by the IFC technique.

## MATERIALS AND METHODS

*Materials*. A peptide corresponding to the effector domain of bovine MARCKS (151−175), the so-called effector peptide, was synthesized as described previously (*17*). Control experiments were performed with another batch of this peptide bought from BIOMOL Research Labs., Inc. (Plymouth Meeting, PA) and showed comparable results. A peptide corresponding to the effector domain of murine MRP (86−109), was synthesized by AMS biotechnology (Lugano, Switzerland). The amino acid composition and the concentration of these peptides were determined by quantitative amino acid analysis. The primary structures of the MARCKS and MRP effector domains are shown in Figure 1. Calmodulin (CaM) from bovine brain was bought from Calbiochem (La Jolla, CA) and stored in 2.5 mM imidazole at pH 7.2. The experiments with CaM were performed in the presence of initially 0.1 mM $CaCl_2$. In a later step, $Ca^{2+}$ was removed by EGTA (ethylene glycol bis($\beta$-aminoethyl ether)-*N*,*N*,*N*′,*N*′-tetraacetic acid). Diphytanoylphosphatidylcholine (DPhPC, MW 846.3) and diphytanoylphosphatidylserine (DPhPS, MW 870.2) were purchased from Avanti Polar Lipids (Alabaster, AL). The lipids, whose purity was >99%, were delivered in chloroform and used without further purification. As buffer, we used 1 mM MOPS (morpholinopropanesulfonic acid) at pH 7.2. The water was deionized (NANOpure, Barnstead, IA) to a specific resistance, >17 MΩ·cm. *n*-Decane was from Fluka (Buchs, Switzerland) and 1-butanol from Merck (Darmstadt, Germany). All measurements were performed at room temperature (about 295 K).

*Black Lipid Membranes*. We used a custom-made Teflon cuvette containing two compartments separated by a Teflon wall with a hole approximately 0.5 mm in diameter. Each compartment has a circular depression for a magnetic stirbar with adjustable speed. Fast stirring, which shortens the lifetime of the membrane, as well as gentle stirring, for which the equilibrium of adsorption is reached only slowly, was avoided. Both compartments contain selfmade Ag/AgCl electrodes. The trans electrode is connected to a current−voltage converter (Keithley 427 Current Amplifier, Cleveland, OH). In the beginning of each experiment, we prepainted the surrounding of the hole with about 1 $\mu$L of a 10 mg/mL (1 wt %) DPhPC/DPhPS lipid solution of the appropriate composition, in *n*-decane. After 20 min we filled each compartment of the cuvette with 5 mL of electrolyte.

We then applied about 1 $\mu$L of the 1 wt % lipid in decane solution on a Teflon loop and painted a membrane. The subsequent thinning of the membranes to a bilayer could be observed optically by a microscope (60-fold magnification) until the membrane turned to a homogeneous black due to the destructive interference from reflections at the front and back interfaces. A more accurate determination of the membrane thickness was obtained by measuring the capacitance of the membrane, which is inversely proportional to the membrane thickness. A signal related to the membrane capacitance was measured by a Gould 450 DSO oscilloscope via the amplitude of the ac current resulting from an applied ac voltage.

*Inner Field Compensation (IFC).* The capacitance of a BLM depends on the voltage across the bilayer (*18*). The voltage at which the capacitance is minimal is equal to the difference between the boundary potentials of both sides of the BLM. Due to voltage-dependent changes in the capacitance, a sinusoidal alternating voltage (ac) at frequency $\omega$ across the bilayer leads to higher harmonics in the capacitive current across the membrane. The amplitude of the signal with frequency $2\omega$ (second harmonic) is proportional to the dc voltage drop in the hydrophobic core of the bilayer (*19*). This voltage drop can originate from intrinsic membrane asymmetries or from an externally applied voltage. Membrane asymmetries stem, for example, from asymmetric ion screening on both sides of the BLM, from asymmetric lipid compositions, or as described in this work, from the adsorption of charged molecules to one side of the membrane.

Our IFC setup (Figure 2A) is adapted from those previously described (e.g. ref *20*). We apply a sinusoidal ac voltage at frequency $f = \omega/2\pi = 1061.9$ Hz and amplitude 30 mV (all ac amplitudes given in rms). The ac voltage was converted from a 3 V direct output by the frequency generator of the lock-in amplifier (SR830 DSP, Stanford Research Systems, Sunnyvale, CA). Thus we could reduce the noise and deformations of the signal delivered by the frequency generator, which provides a maximal ac amplitude of 5 V. A variable dc voltage was added to this ac voltage via a summator which decoupled both sources. At the beginning of each measurement, we apply a dc voltage with a magnitude of about 20 mV. The signal from the membrane (transmembrane current converted to voltage) is fed into the lock-in amplifier, locked to the second harmonic. We then adjust the phase angle $\varphi$ between reference signal and measurement signal at the lock-in amplifier to a value, for which the lock-in amplifier output is zero. Then we switch the phase angle by $\pm 90°$ to adjust the lock-in amplifier to maximal sensitivity. The sign of the phase shift is chosen such that we later obtain a negative feedback in the automatic mode (see below). Next, we change the applied dc voltage to set the output of the lock-in amplifier again to zero. This voltage, which corresponds to the negative intrinsic transmembrane voltage, compensates asymmetries in the membrane itself and is therefore called compensation voltage. Due to the symmetry of the lipid composition and of the electrolyte on both sides of the membrane this value starts at about zero. Finally, we close our feedback circuit by replacing the manually applied dc voltage with the output of the lock-in amplifier (automatic mode). We have chosen the phase angle $\varphi$ such that any change in the intrinsic

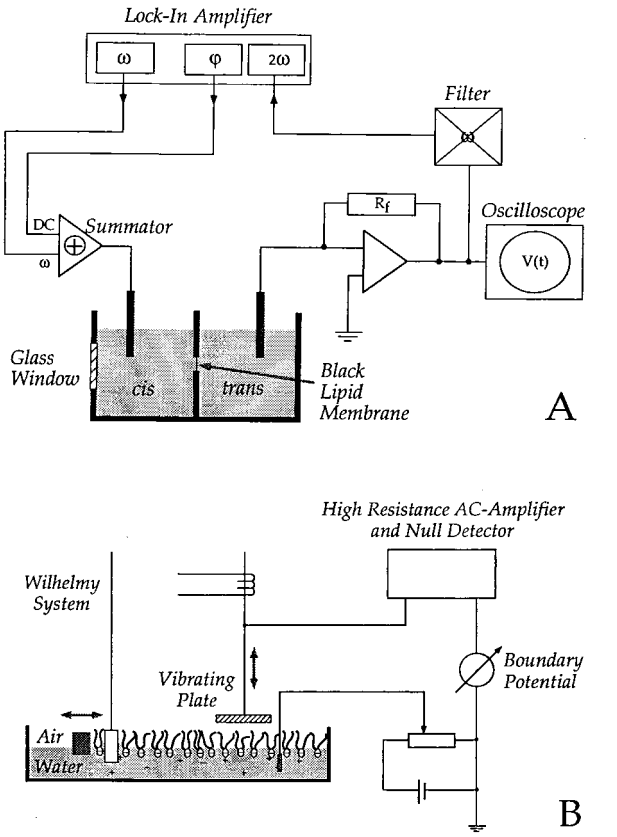


FIGURE 2: (A) Setup of the inner field compensation (IFC) to measure changes in the boundary potential of BLMs. The capacitive transmembrane current is converted to a voltage by the operational amplifier. The filter eliminates the first harmonic component of the signal. The lock-in amplifier is locked to the second harmonic. Amplitude and sign of the DC output depends on the phase $\varphi$ between the second harmonic reference and the measurement signal. The DC output is fed back to the membrane and added to the first-harmonic signal provided by the lock-in amplifier. (B) Setup for the vibrating plate technique (VPT) over a lipid monolayer on a Langmuir trough. The surface pressure is monitored by a Wilhelmy system and can be controlled by the movable barrier on the left side. For more details see Materials and Methods.

transmembrane voltage leads to an output of the lock-in amplifier that compensates for this change (negative feedback). The higher the sensitivity of the lock-in amplifier, the better this compensation voltage corresponds to the negative intrinsic transmembrane voltage. On the other hand, the increase in sensitivity produces an increase in noise and instability of the circuit. We thus measure at sensitivities for which a further increase hardly changes the compensation voltage. The compensation voltage is finally converted into a digital signal by a DigiData 1200 Interface (Axon Instruments, Foster City, CA) and recorded on a 486 PC at an acquisition rate of one point per second using the program pCLAMP6 (Axon Instruments). The data were smoothed with the program EasyPlot (Spiral Software, Brookline, MA) using the sliding data window option. The resolution of the IFC is about 1 mV. The scatter of the plateau values of titrations of different preparations of the cuvette is up to 10 mV. The standard error in our measurements was below 5 mV.

The boundary potential was measured on the trans side of the cuvette, with the cis side as a reference. To compensate for the change in boundary potential due to adsorption of the positively charged MARCKS or MRP

peptides to the cis side of the negatively charged membrane, it is necessary to apply a negative potential to the cis side. To represent the data in form of a positive signal, we show the negative change in the compensation voltage as a function of peptide concentration.

*Lipid Films at the Air−Water Interface.* Lipid monolayers were prepared on a computer-controlled custom-made Langmuir trough (subphase 95 mL, area 5 × 25 $cm^2$). Lipids dissolved in chloroform (∼1 mg/mL) were spread on the surface of the buffered aqueous subphase. After spreading, the chloroform was allowed to evaporate for 15 min. For the adsorption experiments, increasing volumes of a peptide stock solution were injected with a Hamilton syringe underneath a preformed lipid film. The subphase was stirred with two magnetic stirrers, and the pressure of the lipid film was kept constant (isobaric conditions). The isotherms of the pure lipids resembled those previously published (*21*, *22*).

*Vibrating Plate.* Surface potential measurements were made by means of a modified vibrating plate technique (VPT) (KSV Instruments Ltd., Helsinki, Finnland). A schematical setup is shown in Figure 2B. A conducting circular plate (diameter 2 cm) is placed less than 1 mm above the air−lipid interface and vibrates at approximately 60 Hz. The surface potential is measured using an Ag/AgCl electrode connected to the subphase via an agar-containing salt bridge. The conductive bridge prevents the peptides from adsorbing onto the electrode and improves the stability of the signal.

As it vibrates, the plate rapidly changes its distance from the lipid/water surface. This leads to changes in the capacitance and, depending on the voltage between the lipid/water surface and the vibrating plate, to charge flow to and from the capacitor plate. The lipid/water surface is almost at the same potential as the bulk electrode, since the electrolyte is a good conductor. The null detector determines the potential of the bulk electrode necessary to minimize the capacitive current. Applying ±100 mV between the aqueous phase and the vibrating plate, should induce a change of 200 mV in the signal from the null compensation of the VPT. By changing the distance of the vibrating plate to the monolayer surface, we can adjust the sensitivity of the VPT to the point where the change in the output is 200 mV. The resolution of the potential measurements is about 3 mV. The scatter of the plateau values of titrations for different preparations of the monolayer are up to 20 mV. The standard error of our measurements was below 10 mV.

## RESULTS

In a first series of measurements we have investigated the binding of the effector domain of MARCKS to negatively charged lipid membranes. BLMs were formed from a 30% DPhPS/70% DPhPC solution in *n*-decane. With the IFC technique we measured the change in the boundary potential following addition of a peptide corresponding to the effector domain of MARCKS to the cis compartment of the cuvette. Measurements at three different concentrations of KCl (Figure 3) clearly show that the binding of the effector peptide to negatively charged membranes can be detected by the IFC. In the presence of 100 mM KCl (open triangles), the signal is already significantly weaker than at 10 mM KCl

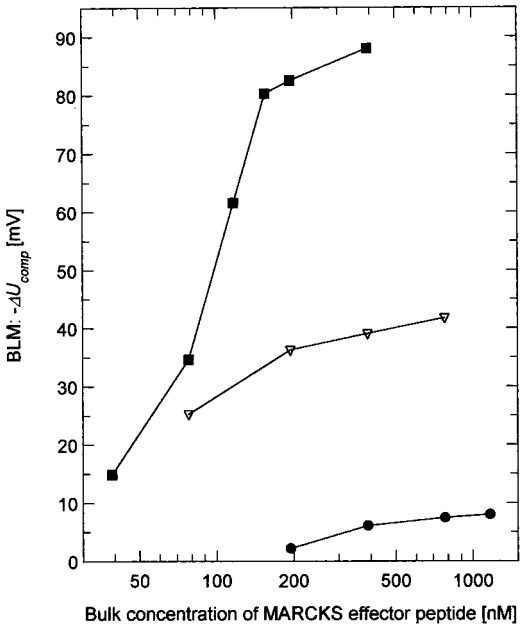


FIGURE 3: Binding of the effector domain of MARCKS to 30% DPhPS/70% DPhPC lipid membranes. Changes in the difference of the boundary potential between the two sides of a BLM upon adsorption of the peptide were measured by IFC for three different concentrations of KCl: 10 mM (■), 100 mM (▽), and 500 mM (●). The buffer was 1 mM MOPS, pH 7.2.

(filled squares). At higher ionic strength (500 mM KCl, filled circles) a significant increase in the compensation voltage in the presence of MARCKS peptide is still observed. It should be noted that the relation between amount of bound peptide and change in boundary potential is nonlinear for surface potentials higher than about 25 mV. The quantitative interpretation of the compensation voltage depends e.g. on the initial surface charge density of the membrane and on the ionic strength of the surrounding electrolyte. We review these points in the Appendix in which we show that, for the conditions of Figure 3, higher changes in the boundary potential correspond to binding of more peptide. The data in Figure 3 show that the interaction of the effector domain with negatively charged membranes decreases as the ionic strength increases. This clearly indicates an electrostatic interaction between the peptide and the membrane, as reported previously (*23*). The remaining signal observed in the presence of 500 mM KCl suggests however that nonelectrostatic interactions also play a role for the binding of the peptide to the membrane. Note, that all curves tend to saturate at higher bulk concentrations of the effector domain. It should be noted, that the comparatively small changes in potential for small bulk concentrations of peptide in the presence of 10 mM KCl are probably due to loss of peptide by adsorption to the walls of the cuvette. The kink in the potential at about 150 nmol bulk concentration of peptide might therefore indicate saturation of the walls of the cuvette with the peptide. In control experiments, we added the peptide in the rear compartment of the cuvette, where there is no glass window for observation of the membrane. Again, one could see a steep increase in the beginning followed by a kink to a smaller slope. The changes in potential were slightly higher compared to addition to the front compartment with the glass window, possibly indicating some loss of peptide to the glass.

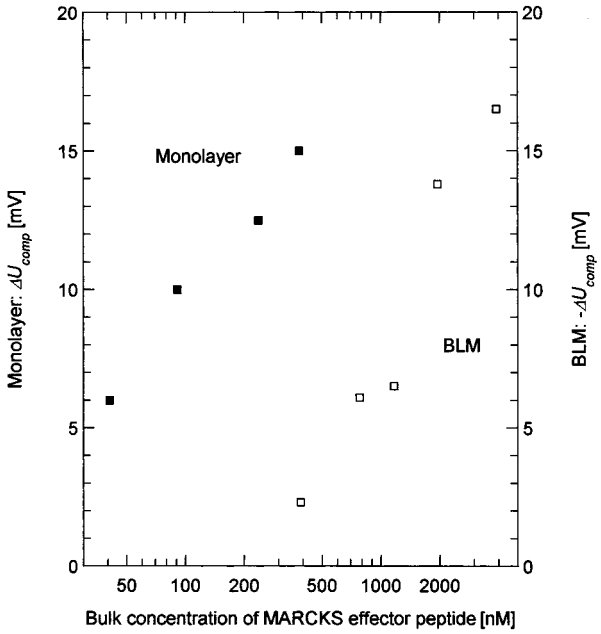


FIGURE 4: Binding of the effector peptide of MARCKS to pure zwitterionic DPhPC membranes. The buffer contained 100 mM KCl and 1 mM MOPS, pH 7.2. Lipid monolayer (■) and the BLM (□) show changes in the boundary potential as measured with VPT and IFC, respectively.

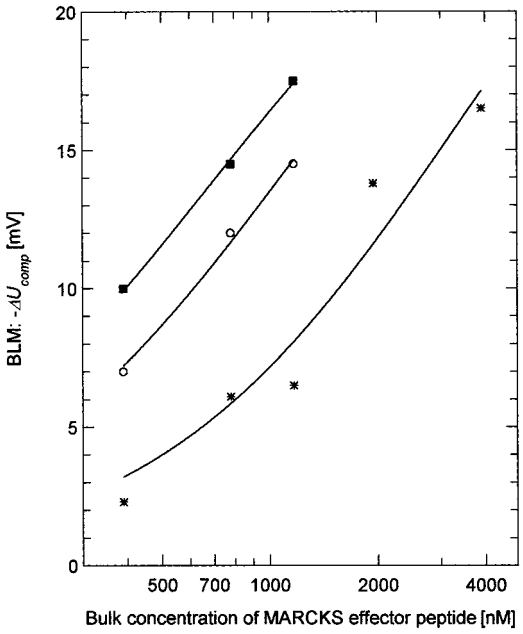


FIGURE 5: IFC results on binding of the effector peptide of MARCKS to BLMs made of pure DPhPC in the presence of three different concentrations of KCl: 10 mM (■), 20 mM (○), and 100 mM (*).

To check whether nonelectrostatic interactions alone can mediate the adsorption of the effector domain of MARCKS to lipid membranes, we performed experiments with zwitterionic DPhPC membranes in the presence of 100 mM KCl. Figure 4 shows that the effector domain also induces changes in the boundary potential of initially uncharged membranes as measured by the IFC. At a concentration of 1 $\mu$M peptide, the signal is however much weaker for the uncharged membrane (about 6 mV) than for the 30% charged membrane (about 40 mV), demonstrating the major contribution of electrostatic interactions to binding. At higher peptide concentrations, we obtain a signal of about 16 mV with no indication of saturation.

To test the adsorption of the peptide to uncharged membranes independently, we also performed measurements with the VPT on a lipid monolayer at a surface pressure of about 30 mN/m. Qualitatively the same results as for the BLM were observed. However, the VPT consistently yields larger changes in the boundary potential upon adsorption of the effector domain to the uncharged membrane. This discrepancy is not necessarily due to different binding mechanisms of the effector peptides to these membranes since we have already observed this phenomenon with other molecules (e.g., pentalysine; manuscript in preparation). Pentalysine is especially interesting as a reference substance, because the amino acid sequence of the effector domain of MARCKS begins with five lysines. Control experiments with the VPT and IFC showed no binding of pentalysine to PC membranes, in agreement with previous results (*24*) and excluding the presence of negatively charged impurities in the lipid (data not shown). We repeated the experiment of Figure 4 with the effector domain of MARCKS from a different supplier (BIOMOL, PA) and could confirm the binding of this peptide to uncharged membranes. Taken together, our data indicate that nonelectrostatic interactions alone cause adsorption of the MARCKS effector domain to lipid membranes. For negatively charged membranes electrostatic interactions are however predominant.

The influence of different bulk concentrations of KCl on the adsorption of the effector domain of MARCKS to pure DPhPC−BLMs is shown in Figure 5. The change in boundary potential is weaker at higher concentrations of potassium. In contrast to the data presented in Figure 3, this observation does not indicate a weaker binding of the peptide. For an initially uncharged membrane the surface potential due to adsorbed charges is expected to be about three times larger in the presence of 10 mM KCl compared to 100 mM KCl in the regime of the Debye−Hückel approximation (for a detailed discussion see the Appendix). Within the error of measurement, the data in Figure 5 correspond to the predictions of the Debye−Hückel theory for the screening of surface charges by monovalent cations. Thus, the amount of adsorbed peptide is about the same for all three concentrations of salt shown in Figure 5. Note also that the signals induced by the peptide in the presence of zwitterionic membranes are similar in magnitude to the signal observed for the same peptide in the presence of negatively charged phospholipid membranes at high salt concentration (compare data for 500 mM KCl in Figure 3 and for 100 mM KCl in Figure 5). This supports the conclusion that the effector domain of MARCKS can adsorb nonelectrostatically to membranes.

In a subsequent series of measurements, we compared the binding of the effector peptides of MARCKS and MRP. Recently, we have shown that binding of the MRP protein to vesicles containing 20% negatively charged lipid is at least 1 order of magnitude weaker than binding of MARCKS protein (*7*, *9*). We have speculated that this difference is due to different structures of the effector domains. As shown in Figure 1, a serine in MARCKS is replaced by a proline in MRP. Moreover one phenylalanine in MARCKS is replaced by a leucine, two lysines are replaced by arginines, and one arginine is missing in MRP. IFC and VPT

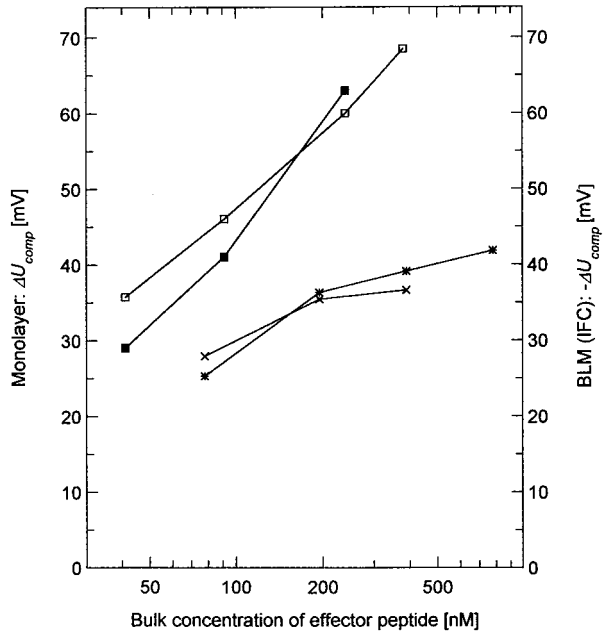


FIGURE 6: Comparison of the binding of the effector peptide of MARCKS and MRP to 30% DPhPS/70% DPhPC membranes at 100 mM KCl. Results of lipid monolayer and BLM measurements with VPT and IFC, respectively. The upper two curves show the monolayer results for the MRP (□) and MARCKS (■) peptide. The lower two curves show the BLM results for the MRP (×) and MARCKS peptide (*).

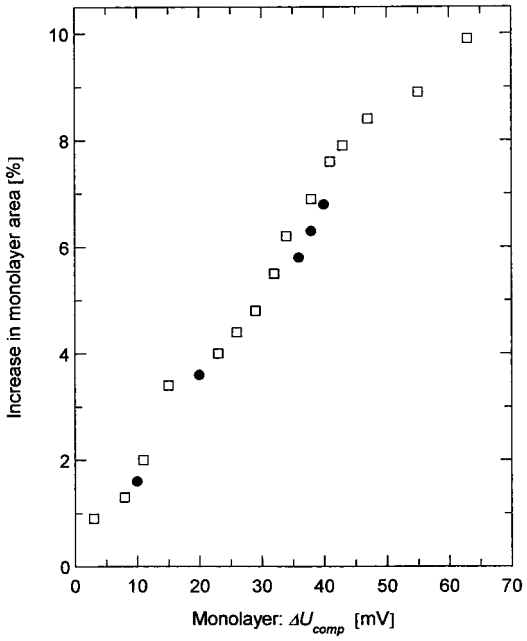


FIGURE 7: Simultaneous recording of the binding of the effector peptides of MARCKS (●) and MRP (□) to 30% DPhPS/70% DPhPC lipid monolayers on a Langmuir trough at 30 mN/m. The increase in area upon insertion is highly correlated with the change in the boundary potential, measured with VPT. The KCl concentration is 100 mM.

measurements on 30% DPhPS/70% DPhPC membranes in the presence of 100 mM KCl do not show significant or systematic differences in the behavior of these peptides within the experimental resolution (Figure 6). Consequently, the decreased affinity of the MRP protein for acidic phospholipid membranes is unlikely to result from differences in the primary sequence of the effector domains of these proteins.

Using two independent techniques, we have monitored simultaneously the binding of the effector domain of MARCKS or MRP to a 30% DPhPS/ 70% DPhPC lipid monolayer in the presence of 100 mM KCl. In addition to the boundary potential, we have also recorded the increase in area of the monolayer at a constant surface pressure of 30 mN/m. The results presented in Figure 7 show that the change in area and the change in potential are highly correlated. Thus adsorption of the peptides to the membrane surface is accompanied by insertion without an indication of saturation for the insertion. Since in this concentration range of peptide, the increase in area is proportional to the amount of bound peptide detected by VPT, the VPT is a valid method to monitor peptide−membrane interactions. Again, no significant difference between the MARCKS and MRP peptides can be seen.

Looking at the kinetic aspect of our measurements we observed that the increase in area was not delayed relative to the increase in boundary potential. This observation shows that the adsorption is rate limiting. Insertion of the peptides must therefore take place within a few seconds after the adsorption. This corresponds to recent measurements on the on and off rates (*25*), where the binding kinetics of MARCKS peptide to lipid vesicles was found to be much faster than 1 s and diffusion limited. In this respect, it is interesting to note that measurements with phloretin showed delays of several minutes between adsorption and insertion (data not shown). In specific cases the combination of a Wilhelmy system and of the VPT is therefore well-suited to discriminate between adsorption and insertion of molecules into membranes. Control measurements with pentalysine showed no insertion into the monolayer (data not shown), in agreement with previous findings (*26*). This result further confirms the conclusion that the effector domains of MARCKS and MRP also interact nonelectrostatically with the membrane by inserting their hydrophobic residues into the membrane.

One mechanism of cellular regulation of the membrane binding of MARCKS and MRP proteins is based on calmodulin (CaM). Recently, the rate constant for the CaM-induced dissociation of a peptide corresponding to the effector domain of MARKCS from lipid vesicles containing small amounts of acidic lipid was determined (*27*). In Figure 8 we show the regulation of the membrane targeting of the effector domain of MARCKS by CaM/$Ca^{2+}$. The figure shows the change in the boundary potential obtained with the IFC upon changing the composition of the bulk phase. At first, in the presence of 10 mM KCl, 1 mM imidazole, and 0.1 mM $CaCl_2$, a BLM was formed from DPhPC/DPhPS (2:1) and the baseline from the IFC was recorded. $CaCl_2$ is necessary to activate CaM so that it can form a complex with MARCKS proteins or peptides corresponding to its effector domain. After 10 min (A), CaM was added to a bulk concentration of 800 nM, to ensure that this concentration of CaM alone has no influence on the membrane potential. At B, 45 min after beginning of the measurement, a peptide corresponding to the effector domain of MARCKS was added to a bulk concentration of 200 nM. Due to the 4-fold excess of CaM, a complex of CaM and MARCKS peptide is rapidly forming thus preventing binding of the protein to the membrane. After 85 min (C), EGTA was added to a bulk concentration of 1 mM to remove calcium

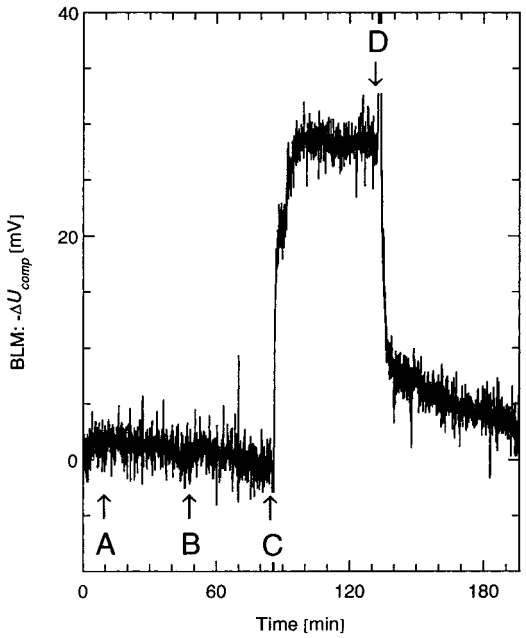


FIGURE 8: Regulation of the adsorption of the effector peptide of MARCKS to BLMs made of 30% DPhPS/70% DPhPC by CaM and $Ca^{2+}$. The buffer contained 10 mM KCl, 1 mM imidazole, and 0.1 mM $CaCl_2$ and was adjusted to pH 7.2. The figure shows the change in compensation voltage of the IFC upon changing the composition of the bulk solution. At time A, CaM was added to a bulk concentration of 800 nM to the cis compartment. At time B, MARCKS peptide was added to a bulk concentration of 200 nM to the cis compartment. At time C, EGTA was added on both compartments of the cuvette to a bulk concentration of 1 mM. At time D, $Ca^{2+}$ was added on both sides to a bulk concentration of 1.2 mM on both sides of the membrane.

ions from the CaM, which brings the CaM into the unactivated form and induces dissociation of the complex with the MARCKS peptide. After dissociation from the complex, the MARCKS peptide rapidly binds to the membrane, changing the compensation voltage of the IFC. As EGTA is also removing calcium ions from the bulk thereby changing the surface potential, EGTA was added symmetrically to both sides of the membrane. After 130 min (D), $CaCl_2$, was (again symmetrically) added to a bulk concentration of 1.2 mM. The excess calcium ions activate CaM, which again forms a complex with the MARCKS peptide, removing the peptide from the membrane and restoring the initial symmetry of the membrane. This experiment shows that CaM/$Ca^{2+}$ can regulate the association of the MARCKS peptide to membranes.

## DISCUSSION

In this paper we study the mechanisms of binding of peptides corresponding to the effector domain of MARCKS and MRP, using IFC for BLMs and VPT and a Wilhelmy system for lipid monolayers in a Langmuir trough. The IFC and VPT make it possible to monitor biologically relevant processes in the vicinity of the membrane which are accompanied by changes in the boundary potential. These include phenomena such as adsorption, desorption, and translocation of molecules as well as changes in the structure of the membrane.

In particular, we have shown that electrostatic forces dominate the interaction of peptides corresponding to the effector domain of MARCKS and MRP to negatively charged membranes. We have also shown that the effector domain of MARCKS and MRP can bind weakly to zwitterionic membranes. Since the binding of the MARCKS peptides is accompanied by partial insertion of the peptide into the membrane, these data demonstrate that the hydrophobic residues in the effector peptide contribute to binding by inserting into the membrane. Under comparable conditions, Glaser and co-workers (*27*) have found an increase in monolayer area of 4% only, instead of 10% in our hands upon insertion of the MARCKS effector peptide into the monolayer. The very high correlation between the increase in area of the monolayer and the change in boundary potential proved that the boundary-potential change is directly related to the binding of these peptides to lipid membranes.

In our experiments, we could not detect a significant difference in the binding behavior between the effector domains of MARCKS and MRP. This is surprising, since for the whole protein a significant difference in the binding to lipid membranes was observed (*7, 9*).

Using IFC, we could also show that calcium can regulate the translocation of the MARCKS effector peptide between CaM in the bulk and the membrane. This experiment sets the basis for in vitro experiments in which signal transduction pathways can be investigated at the water−membrane interphase. Note that for binding processes, the temporal resolution of both methods is limited by the diffusion of membrane active substances from the bulk to the membrane surface. However, the time resolution for a nondiffusion-limited process which changes the electrostatic properties of a peptide or protein at the membrane (e.g., phosphorylation of membrane-bound MARCKS protein) is in the range of a few seconds.

The BLM and the lipid monolayer on the Langmuir trough, as well as liposomes, are models for biological membranes. In comparison with liposomes, one advantage of the BLM and the Langmuir trough is a much higher ratio of bulk volume to membrane surface. Therefore, the peptide bulk concentration does not change significantly upon adsorption of the peptide to the membrane. Also adsorption to Teflon walls is often less problematic compared to the glass cells used in $\zeta$ potential measurements. For small concentrations of peptide however, adsorption of peptide might also be a problem in our BLM measurements as can be seen in Figure 3 for 10 mM KCl. The slope of these data is very steep at low concentrations of peptide, possibly due to a significant reduction of the bulk peptide concentration caused by adsorption to the membrane and the walls of the cuvette. The use of a single membrane can also avoid the problem of nonspecific membrane−membrane interactions which may impair the study of peptide−lipid interactions in liposome experiments. Further advantages of BLMs are that they can be prepared asymmetrically and that the translocation of biologically relevant molecules through the membrane (*28*) and the formation of channels can be measured. The influence of proteins and polymers on the stability of BLM can be studied by rupture experiments (*29*). Lipid monolayers in a Langmuir trough, on the other hand, allow the study of the influence of surface pressure on the binding of membrane-active molecules. For a peptide inserting into a membrane, the binding can be monitored by the VPT as a potential change and simultaneously by an increase in area of the monolayer under isobaric conditions. From a practical

point of view, the methods of IFC and VPT have the advantage that labeling of lipids or peptides is not necessary. The IFC and VPT are especially suited to detect minute changes in the surface−charge density: For example, starting with a neutral membrane at 100 mM KCl, the condensation of a single charge per 100 lipid molecules gives a surface potential of about 3 mV. Assuming a typical membrane surface of 1 $mm^2$ for our BLM this corresponds to binding of about 20 fmol singly charged molecules.

## ACKNOWLEDGMENT

We want to express our gratitude to Dr. Yuri A. Ermakov from the A.N. Frumkin Institute of Electrochemistry in Moscow (Russia), who previously established the setup of the IFC in our lab. We would like to thank Professor Joel A. Cohen (Department of Physiology and Biophysics; University of the Pacific, San Francisco) for stimulating discussions and careful proofreading of the manuscript. Moreover we want to thank the workshop of our department for constructing and building the devices mentioned in the text. For his support we would like to thank Professor Gerhard Schwarz.

## APPENDIX

In this section we discuss how the changes in boundary potential can be evaluated to determine binding affinities. According to the Gouy−Chapman theory, the surface potential $\psi$ at the membrane/water interface for a fixed homogeneously smeared surface charge density $\sigma$ in the presence of a 1:1 electrolyte (e.g., KCl) with a concentration of $n_0$ ions per unit volume is given by (*30*)

$$\psi = \frac{2kT}{e}\sin h^{-1}\left(\frac{\sigma}{\sqrt{8\epsilon_0\epsilon_w kTn_0}}\right) \qquad \text{(A1)}$$

where $k$ is the Boltzmann constant, $T$ the temperature, $e$ the elementary charge, $\epsilon_0$ the dielectric constant of the vacuum, and $\epsilon_w \approx 80$ the relative dielectric constant of water. Equation A1 does not include screening of charges by the peptide, binding of monovalent cations, or changes in the dipole potential. Due to these assumptions, Equation A1 can be explicitly inverted, and the surface charge density can be expressed as a function of the measured potential. The change in surface potential is then directly related to the surface density of the bound peptide, provided that the number of surface charges compensated by a single adsorbed peptide is known. Binding curves can be obtained by plotting the variation in surface charge density vs the bulk concentration of peptide. For each point of the binding curve an apparent binding affinity of the peptide can be defined, e.g., by dividing the surface density of bound peptide by the bulk concentration.

The advantage of the IFC and VPT is that they directly measure changes in the electric potential upon binding of peptides. Therefore, in Figures 3−8, we showed the changes in the boundary potential instead of the concentrations of bound peptide. Under several assumptions the measured changes in surface potential can be used to quantify the surface bound peptide. Below we discuss this in more detail.

In the limit of very high and very low surface-charge densities, the interpretation of changes in electric potential with respect to binding can be simplified. First we discuss the case of low surface-charge densities. In the Debye−Hückel approximation, valid for surface potentials below 25 mV, the surface potential $\psi$ is linear with respect to the Debye screening length:

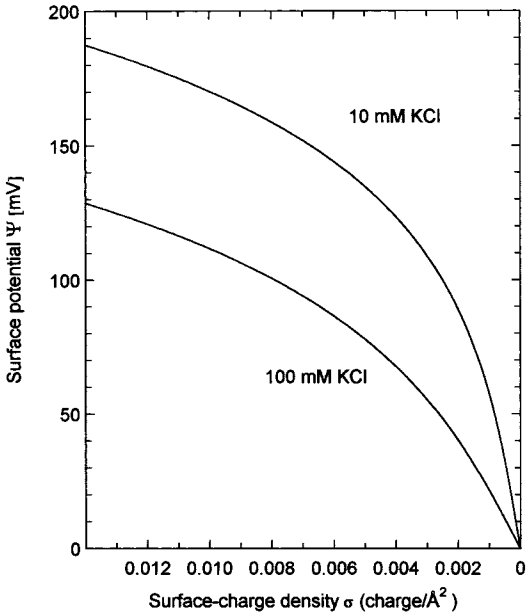


FIGURE 9: Dependence of the absoute value of the surface potential on the absolute value of the surface-charge density according to the Gouy−Chapman theory. Note that the absolute value of the surface charge density decreases from left to right. A pure PS membrane (area per lipid 70 $Å^2$) corresponds to 0.014 charges per $Å^2$.

$$\psi = \frac{\sigma}{\epsilon_0\epsilon_r}\lambda_D \qquad \text{(A2)}$$

The screening length depends on the concentration of ions in the electrolyte and is given by

$$\lambda_D = \left(\frac{\epsilon_r\epsilon_0 kT}{e^2 n_0}\right)^{1/2} \qquad \text{(A3)}$$

This shows that the surface potential for a fixed surface-charge density (amount of bound peptide) is higher at lower concentrations of KCl (Figure 5). Adsorption of a charged peptide to an initially uncharged membrane will induce a screening-dependent surface potential. By using eqs A2 and A3, this surface potential can be related in linear approximation to the surface charge density of the adsorbed peptide.

Adsorption of a basic peptide to a negatively charged membrane reduces the surface-charge density. This can be seen in Figure 9, where the surface potential is shown as a function of the surface-charge density for two different salt concentrations (for a PS membrane both values are negative, but we consider absolute values). The surface-charge density on the abscissa decreases from left to right, which corresponds to the titration curves in Figures 3 and 6, where higher bulk concentrations of peptide correspond to smaller surface charge densities. Starting in Figure 9 from left with one charge per lipid area (70 $Å^2$), corresponding to a surface-charge density of 0.014 charges/$Å^2$, the two curves for 10 and 100 mM KCl are at the beginning almost parallel. In other words, the same changes in surface potential correspond

to the same changes in surface-charge concentration, for both KCl concentrations. In the presence of a highly charged membrane, the measured surface potential is therefore approximately a binding signal. This is the limiting case of high surface-charge densities. Note that although the surface potential has initially a high value on both sides of the membrane, the compensation voltage of IFC is zero in the beginning of the titration due to symmetrical conditions. Strictly speaking, all of the assumptions of the Gouy−Chapman theory have to be applicable when using this theory to estimate binding of charged peptides to membranes. Nevertheless, the Gouy−Chapman theory has been applied by many groups quite successfully to a number of adsorption processes, although not all conditions were fulfilled. In the following we give an example of how we evaluate our data semiquantitatively in terms of binding and discuss the limitations and validity of our approach.

In Figure 3, due to the 30% charged lipids in the membrane, we start with an intermediate surface potential of about 130 mV for 10 mM KCl and about 70 mV for 100 mM KCl on both sides of the BLM. Binding of peptides to this membrane results in changes of the surface potential which depend on the KCl concentration; thus the potential curves for the two salt concentrations are not parallel in this surface-charge density range (Figure 9). Therefore we have to estimate the change in surface-charge density from the change in surface potential for both concentrations of KCl separately, with the help of Figure 9. This analysis shows that the higher change in the surface potential for 10 mM KCl corresponds to more binding of peptide, as stated in the Results.

In the previous paragraph we used the Gouy−Chapman theory and assumed that each peptide neutralizes charges at the membrane surface upon binding. In the following section we give some ideas on how this approach can be refined.

First, we did not take changes of the dipole potential into account. For example, binding of the peptide can lead to structural changes of the membrane. Also, the membrane-inserting parts of the peptide, i.e., the hydrophobic residues, could have dipole moments different from the lipid molecules they displace. Moreover, binding could be accompanied by changes in the water structure in the headgroup region of the lipids (*31*, *32*). All three effects can alter the effective dipole potential of the membrane. Inspection of Figure 5 shows that the modification in the boundary potential with increasing monovalent salts follows the Deybe−Hückel approximation nicely. This indicates that in this case no changes in the dipole potential occurred, provided that the amount of bound peptide remained constant.

Another possibility to evaluate the contribution of dipole potential changes to our signal is to compare the results obtained with VPT and IFC with results obtained with other techniques that are sensitive to the surface potential alone. For example, conductance probes for BLMs (*33*) or $\zeta$ potential measurements for lipid vesicles (*23*). Although theoretically possible, in practice surface−potential measurements on different model systems lead to different results. With the $\zeta$ potential technique, for example, the surface potential has to be calculated from the measured potential at the hydrodynamic plane of shear to the surface of the membrane, which introduces an additional parameter: the distance of this hydrodynamic plane of shear from the membrane surface. Recently, the dipole potential for lipid bilayers was also measured with fluorescent probes (*34*, *35*). The disadvantage of this method is that the fluorescent probes change the dipole potential of the membrane.

The monolayer results correspond qualitatively to the IFC data. Nevertheless, the monolayer measurements always show larger changes in the boundary potential. One quantity which can influence the results of the VPT on monolayers is the surface pressure of the lipid film. The literature reports a variety of so-called "bilayer equivalence-pressures" (*36*−*39*). They are usually only valid for one type of membrane system, and therefore there seems to be no general equivalence pressure. We chose the widely used 30 mN/m (*40*).

Both for the lipid monolayer and the BLM, an increase in area upon insertion of a peptide leads to a different surface charge density of the lipid headgroups, which can induce a change in the surface potential, irrespective of the charge of the inserting peptide. In Figure 7, we saw an increase of 10% in monolayer area for the highest amount of bound peptide. In contrast to other reports (e.g., ref *41*) we performed isobaric, instead of isochoric, measurements on the lipid monolayer, because this more nearly resembles the conditions found in BLMs in which lipids can be transferred into the annulus upon insertion of peptides into the membrane.

Binding of the monovalent cations to the membrane (in addition to screening) and screening of charges by the peptides (in addition to binding) also modify the surface potential. Such effects cannot be explained by the Gouy−Chapman theory. Binding constants for various monovalent cations have been determined, but the values are small and several values have been published (*42*). A different approach to take condensation of counterions in the electric double layer into account was suggested recently (*43*). Provided that the peptide exerts a screening effect like a multivalent point charge, screening by peptides can be estimated with the Gouy−Chapman theory. Considering the entire MARCKS peptide with 13 charges as a simple screening ion, the Gouy−Chapman theory predicts an unreasonably high peptide concentration at the membrane surface and thus an enormous screening effect. It is therefore necessary to consider the spatial distribution of the charges, and effective charges usually are introduced (*44*).

## REFERENCES

1. Sakmann, B., and Neher, E., Eds. (1983) *Single-channel recording*, Plenum Press, New York.
2. McLaughlin, S. (1989) *Annu. Rev. Biophys. Biophys. Chem. 18*, 113−136.
3. McLaughlin, S., and Aderem, A. (1995) *Trends Biochem. Sci. 20*, 272−276.
4. Vergères G., Manenti, S., and Weber, T. (1995) *Signaling Mechanisms: From Transcription Factors to Oxidative Stress* (Packer, L., and Wirtz, K. W. A., Eds.) Vol. H92, pp 125−137, Springer-Verlag, Berlin.
5. Aderem, A. (1992) *Cell 71*, 713−716.
6. Blackshear, P. J. (1993) *J. Biol. Chem. 268*, 1501−1504.
7. Vergères, G., Manenti, S., Weber, T., and Stürzinger, C. (1995) *J. Biol. Chem. 270*, 19879−19887.
8. Qin, Z., and Cafiso, D. S. (1996) *Biochemistry 35*, 2917−2925.
9. Vergères, G., and Ramsden, J. J. (1998) *Biochem. J. 330*, 5−11.
10. Erne, D., Sargent, D. F., and Schwyzer, R. (1985) *Biochemistry 24*, 4261−4263.

11. Sargent, D. F., Bean, J. W., and Schwyzer, R. (1989) *Biophys. Chem. 34*, 103−114.
12. Gevod, V. S., and Birdi, K. S. (1984) *Biophys. J. 45*, 1079−1083.
13. Nicolay, K., Sautereau A.-M., Tocanne, J.-F., Brasseur, R., Huart, P., Ruysschaert, J.-M., and de Kruijff, B. (1988) *Biochim. Biophys. Acta 940*, 197−208.
14. Gabev, E., Kasianowicz, J., Abbott, T., and McLaughlin, S. (1989) *Biochim. Biophys. Acta 979*, 105−112.
15. Duplaa, H., Convert, O., Sautereau, A.-M., Tocanne, J.-F., and Chassaing, G. (1992) *Biochim. Biophys. Acta 1107*, 12−22.
16. Pickar, A. D., and Benz, R. (1978) *J. Membr. Biol. 44*, 353−376.
17. Taniguchi, H., and Manenti, S. (1993) *J. Biol. Chem. 268*, 9960−9963.
18. Babakov, A. V., Ermishkin L. N., and Liberman, E. A. (1966) *Nature 210*, 953−955.
19. Carius, W. (1976) *J. Colloid Interface Sci. 57*, 301−307.
20. Sokolov, V. S., and Kuz'min, V. G. (1980) *Biophysics 25*, 174−177.
21. Evans, R., Williams, M., and Tinoco, J. (1987) *Biochem. J. 245*, 455−462.
22. Demel, R. A., Paltauf, F., and Hauser, H. (1987) *Biochemistry 26*, 8659−8665.
23. Kim, J., Blackshear, P. J., Johnson, J. D., and McLaughlin, S. (1994) *Biophys. J. 67*, 227−237.
24. Kim, J., Mosior, M., Chung, L. A., Wu, H., and McLaughlin, S. (1991) *Biophys. J. 60*, 135−148.
25. Arbuzova, A., Wang, J., Murray, D., Jason, J., Cafiso, D. S., and McLaughlin, S. (1997) *J. Biol. Chem. 43*, 27167−27177.
26. Ben-Tal, N., Honig, B., Peitzsch, R. M., Denisov, G., and McLaughlin, S. (1996) *Biophys. J. 71*, 561−575.
27. Glaser, M., Wanaski, S., Buser, C. A., Boguslavsky, V., Rashidzada, W., Morris, A., Rebecchi, M., Scarlata, S. F., Runnels, L. W., Prestwich, G. D., Chen, J., Aderem, A., Ahn, J., and McLaughlin, S. (1996) *J. Biol. Chem. 271*, 26187−26193.
28. Pohl, P., Rokitskaya, T. I., Pohl, E. E., and Saparov, S. M. (1997) *Biochim. Biophys. Acta 1323*, 163−172.
29. Klotz, K.-H., Winterhalter, M., and Benz, R. (1993) *Biochim. Biophys. Acta 1147*, 161−164.
30. Hiemenz, P. C. (1986) *Principles of colloid and surface chemistry*, p 702, Marcel Dekker Inc., New York.
31. Simon, S. A., and McIntosh, T. J. (1989) *Proc. Natl. Acad. Sci. U.S.A. 86*, 9263−9267.
32. Parsegian, V. A., Rand R. P., and Rau D. C. (1995) *Methods Enzymol. 259*, 43−95.
33. Cohen, J. A., and Moronne, M. M. (1978) *Biochem. Biophys. Res. Commun. 83*, 1275−1283.
34. Malkov, D. Yu., and Sokolov V. S. (1996) *Biochim. Biophys. Acta 1278*, 197−204.
35. Clarke, R. J. (1997) *Biochim. Biophys. Acta 1327*, 269−278.
36. Albrecht, O., Gruler, H., and Sackmann, E. (1978) *J. Phys. 39*, 301−313.
37. Nagle, J. (1980) *Annu. Rev. Phys. Chem. 31*, 157−195.
38. Gruen, D. W. R., and Wolfe, J. (1982) *Biochim. Biophys. Acta 688*, 572−580.
39. MacDonald R. C., and Simon S. A. (1987) *Proc. Natl. Acad Sci. U.S.A. 84*, 4089−4093.
40. Blume, A. (1979) *Biochim. Biophys. Acta 557*, 32−44.
41. Kennedy, M. T., Brockman, H., and Rusnak, F. (1997) *Biochemistry 36*, 13579−13585.
42. Ermakov, Yu. A. (1990) *Biochim. Biophys. Acta 1023*, 91−97.
43. Attard, P. (1995) *J. Phys. Chem. 99*, 14174−14181.
44. Stankowski, S. (1991) *Biophys. J. 60*, 341−351.

BI981765A